

FEM Analysis of Cage Stress Distribution: Part1: Cylindrical Roller Bearing

A. Dib and A. Haiahem

Laboratoire de Mécanique Industrielle (LMI), Annaba University, Algeria

Abstract: This study reports on a numerical study of cylindrical roller cage. The analysis is based on finite element method. The results show that traction stress is the cause of the failure of the cage. Stress concentration is located in the edge of the hole of the cage. The compressive stress lies in the Y direction but does not cause damage. The most effect of cage damage is the traction stress in the edge of the cage.

Key words: Cylindrical roller bearing, tribology, stress, FEM

INTRODUCTION

Practical rotor systems subjected to relatively large radial loads are often supported by roller bearings primarily due to the large load support and stiffness characteristics of such bearings. Many studies have been performed in the purpose to understand the governing mechanisms of roller bearing.

Dowson and Higginson^[1] have suggested that considerable cage roller slip could be expected in lightly loaded roller bearings. Harris^[2] achieved considerable success in correlating theoretical and experimental values of cage speed. However, few studies have investigated dynamic cage motion for cylindrical roller bearings. A particular interest is Gupta's study^[3] investigating the effect of race-cage and roller cage pocket clearance on cage motion. Nelias^[4] has developed a new model which predicts and locates power losses in a high-speed cylindrical roller bearing, operating under radial load. Results show that the power loss is significant in the interaction cage-ring and roller cage. A recent work^[5,6], cage instability has been studied as a function of the roller-race and roller cage pocket clearances light-load and high-speed condition. The results indicate that the cage exhibits stable motion for small values of roller-race and roller-cage pocket clearance.

The aim of the current investigation is to provide a better understanding of the stress distribution in cylindrical roller bearing cage using Finite Element Method (FEM).

GOVERNING EQUATIONS

As shown schematically in Fig. 1, the dominant velocity for the roller/cage will be the roller velocity about

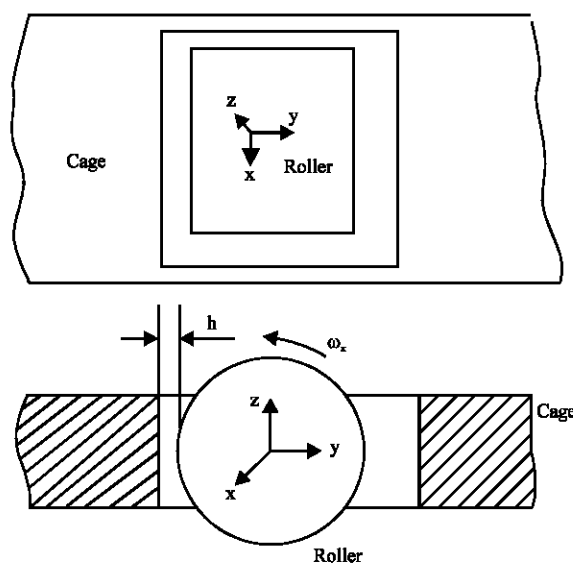


Fig. 1: Hydrodynamic interaction between the cage and the roller

x axis. It will be assumed all the hydrodynamic action takes place on the cylindrical surface only and the end faces are free of any forces.

The maximum pressure is obtained by using Martin theory. The global balance of the cylindrical roller bearing was not taking into account. The study focus in the local interaction between the cage and roller.

Analysis of this contact involved solution of the one-dimensional Reynolds equation in direction of slip and integration over the contact area to obtain total load.

The assumptions used in the analysis are:

- The surfaces are essentially rigid and circular and the spacing between them can be presented by a parabolic approximation.

- A full film lubricant exists between the surfaces.
- The lubricant is Newtonian with a constant viscosity.

The Reynolds equation is written as

$$\frac{\partial}{\partial x} \left(h^3 \frac{\partial p}{\partial x} \right) = 6\mu(u_1 + u_2) \frac{\partial h}{\partial x} \quad (1)$$

Since the contact is Hertizian, Reynolds equation become

$$\frac{\partial p}{\partial x} = 6\mu(u_1 + u_2) \frac{h - h^*}{h^3} \quad (2)$$

$$h = h_0 + \frac{x^2}{2R_x} \quad (3)$$

The contact area was subjected to the following boundary conditions:

$$p=0 \text{ for } x = x_o \text{ and } p = \frac{\partial p}{\partial x} = 0 \text{ for } x = x_i$$

where

x_i the abscise of the inlet contact

x_o the abscise of the outlet contact

Putting

$$h = h_0 \left(1 + \frac{x^2}{2R_x h_0} \right) = h_0 (1 + \text{tg}^2 \phi) \quad (4)$$

where

$$\text{tg} \phi = \frac{x}{\sqrt{2R_x h_0}} \quad (5)$$

Finding the pressure lead us to resolve the following integral

$$p = \int_{\phi_s}^{\phi} \frac{6\mu(u_1 + u_2)\sqrt{2R_x h}}{h_0^2} \cdot \frac{1 + \text{tg}^2 \phi - \frac{h^*}{h}}{(1 + \text{tg}^2 \phi)} d\phi \quad (6)$$

$$p(\phi) = \int_{\phi_s}^{\phi} \frac{6\mu(u_1 + u_2)\sqrt{2R_x h_0}}{h_0^2} \cdot \left(\cos^2 \phi - \frac{h^*}{h_0} \cos^4 \phi \right) d\phi \quad (7)$$

$$\text{with } \frac{1}{\cos^2 \phi} = 1 + \text{tg}^2 \phi \quad (8)$$

$$\cos^2 \phi \cdot d\phi = \frac{\phi}{2} + \frac{\sin^2 \phi}{4}$$

$$\cos^4 \phi \cdot d\phi = \frac{3\phi}{8} + \frac{\sin^2 \phi}{4} + \frac{\sin^4 \phi}{32} \quad (9)$$

The pressure between solids can be written as:

$$p = \frac{6\mu(u_1 + u_2)\sqrt{2R_x h_0}}{h_0^2} \cdot \left\{ \left(\frac{\phi}{2} + \frac{\sin^2 \phi}{4} + \frac{\pi}{4} \right) - \frac{h^*}{h_0} \left(\frac{3\phi}{8} + \frac{\sin^2 \phi}{4} + \frac{\sin^4 \phi}{32} + \frac{3\pi}{16} \right) \right\} \quad (10)$$

The boundary condition in outlet contact can be written as :

$$\begin{aligned} & \left(\frac{\phi_s}{2} + \frac{\sin^2 \phi_s}{4} + \frac{\pi}{4} \right) - \frac{h^*}{h_0} \left(\frac{3\phi_s}{8} + \frac{\sin^2 \phi_s}{4} + \frac{\sin^4 \phi_s}{32} + \frac{3\pi}{16} \right) = 0 \\ & 1 - \frac{h^*}{h_0} \cdot \cos^2 \phi = 0 \end{aligned} \quad (11)$$

After computing, one has

$$\text{tg} \phi_s = 0.475 \quad \text{and} \quad x_s = 0.475 \sqrt{2R_x h_0} \quad (12)$$

$$\frac{h^*}{h_0} = 1.226$$

The maximum pressure is given by Eq. 13

$$p_{max} = 0.76 \frac{\mu(u_1 + u_2)\sqrt{2R_x h_0}}{h_0^2} \quad (13)$$

Integrating the pressure Eq. 7

$$\frac{W}{L} = \int_{\phi_s}^{\phi} p(x) dx = \frac{6\mu(u_1 + u_2)\sqrt{2R_x h_0}}{h_0^2} \int_{\phi_s}^{\phi} f(\phi) \sqrt{2R_x h_0} (1 + \text{tg}^2 \phi) d\phi \quad (14)$$

Total linear load supported by the contact is :

$$\frac{W}{L} = 2.448 \frac{\mu(u_1 + u_2) R_x}{h_0} \quad (15)$$

OPERATING CONDITIONS

The material of the cage is the bronze. The roller is cylindrical and his material is 10Cr6. The dimension of the cage and the load applied are shown in Table 1.

Table 1: Operating condition of the cage

Dimension and load	Values
Axial length of cylindrical roller, L	14 (mm)
Diameter of cylindrical roller, $2R_w$	12 (mm)
Axial length of cage, L_c	14.35 (mm)
Radial length of cage, D_c	12.6 (mm)
Radial load, Q_r	150 000 N
Lubricant viscosity, μ	0.01 (N s m^{-2})
Angular roller velocity, $\dot{\omega}_r$	170 283 (rpm)

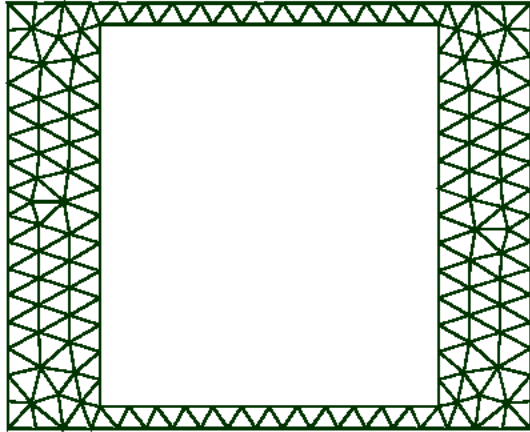


Fig. 2: Mailed cage

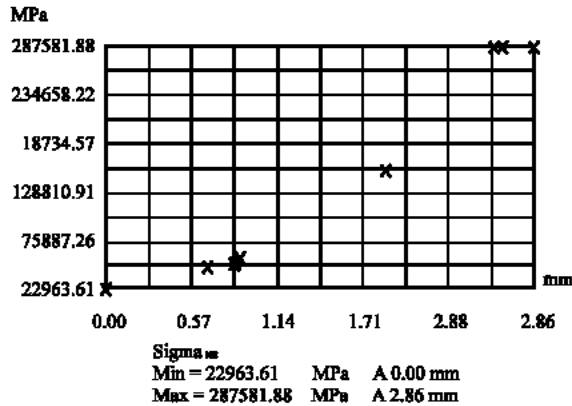


Fig. 3: Stress distribution in the edge

RESULTS AND DISCUSSION

The area is divided into 242 elements and 182 nodes as shown in Fig. 2. The code used in this study is RDM6. The variation of the traction stress in direction of the traction force is shown in Fig. 2. It is obvious that the stress rises in the edge of the cage. The stress traction σ_{xx} exceed the value of young modulus, causing a plastic deformation in the edge of the cage. The magnitude of the damage is shown in Fig. 4. The compressive stress is located in the middle of the cage in the opposite of the axial direction and their magnitude is less than young modulus. According to Fig. 4, the edge of the cage is

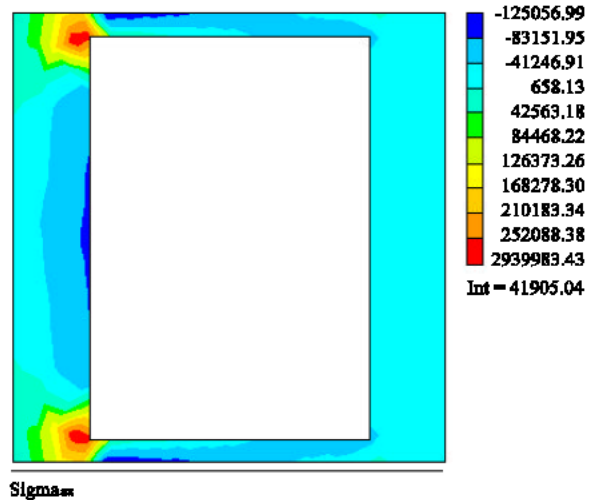


Fig. 4: Stress distribution in the whole cage

subjected to a traction stress in x direction. The value of this stress is higher than elastic modulus, so the can be deformed in this area.

CONCLUSION

The results show that traction stress is the cause of the failure of the cage. Stress concentration is located in the edge of the hole of the cage. The compressive stress lies in the Y direction but does not cause damage. The most effect of cage damage is the traction stress in the edge of the cage.

REFERENCES

1. Dowson, D. and G.R. Higginson.,1963. Theory of roller bearing, lubrication and deformation' Lubricated and wear convention. Institution of mechanical engineers, London.
2. Harris, T.A., 1966. An analytical method to predict skidding in high speed roller bearings. Trans. Of the a American Society of l Lubrication Engineers, pp: 229.
3. Gupta, P.K., 1991. Modeling of instabilities induced by cage clearances in cylindrical roller bearing. STLE Tribology Trans., 34: 1-8.
4. Nelias, D., J. Seabra, L. Flamand and G. Dalmaz, 1994. Power loss prediction in high speed roller bearing. Dissipative Processes in Tribology, pp: 465-478.
5. Niranjana, G., R.W. Carl and S Farshid, 2004. Cage instabilities in cylindrical roller bearings. ASME J. Tribol., 126: 681-689.
6. Neng, L.T. and L.J. Fin, 2002. Ball bearing skidding under radial and axial loads. Mechanism and machine Theory, 37: 91-113.